している。また，サブクローンを作製した場合，オリジナルのクローン番号とサブクローン番号の両方を含むよう命名するべきであるとも提言している。現在，世界中の研究室でiPS細胞の樹立が進められており，その株数は数年のうちに数万という値に達することが予想される。シリアル番号やIDをつけていくとしたら，このような莫大な細胞株数に対応できるものでなければならない。アラビア数字のみではなく，アルファベットなどの文字や記号とアラビア数字を組み合わせてIDを表記すれば，細胞株数が膨大になっても対応できるのではないかと山中所長ら[4]は提案している。

ヒトES/iPS細胞の既存の細胞株について

山中所長ら[4]は，すでに世界中に広く知られている細胞株(例：201B7, hFIB2-iPS2)に新規にシリアル番号等で設定し直す場合にも，オリジナルの名称およびクローンIDを継承することができるような柔軟性をもたせるべきであると提言している。オリジナルの名称から細胞株の情報や原著論文を簡単に収集できるなど，研究者にとって都合が良い点が多いとしている[4]。すでに独自の方式で命名し，細胞株を管理している研究機関は多いため，すべての研究機関の樹立細胞株に対して公平にIDを分配するには多くの困難が予想される。しかし，集積された細胞情報や研究成果を活用するためにも，国際規格のIDを公平に付与できるよう整備し，細胞株のデータベース化を推進していく必要があるのではないだろうか。

すべての多能性幹細胞へ適応

ISCRの提案は，**図**の(c)の部分には，“i”あるいは“e”を表記することによりその細胞株がヒトiPS細胞株とヒトES細胞株のいずれかであることを識別できるようにするというものである[3]。この点に関して，山中所長らとPollok所長ら両者ともに，マウスiPS細胞，体細胞核移植ES細胞(NT-ESC)，単為発生胚由来ES細胞(parthenogenetic-ESC)，胚性腫瘍細胞(embryonal carcinoma cell：ECC)，胚性生殖系細胞(embryonal germ cell：EGC)，エピブラスト幹細胞(epiblast stem cell：EpiSC)などの多能性細胞をすべてこの命名法規定の対象に含めるべきであり，これらを正確に識別できるよう動物種や由来細胞を表すコードを**図**の(c)に表記することを提案している[4][5]。しかし，筆者らは，細胞種を識別するコードを頭につけたほうが分類しやすいのではないかと考える(**図**)。

ヒトES/iPS細胞において特定の病名を表すのは適当ではない

名称に病名を含めることに関して，Pollok所長ら[5]は懸念を抱いている。多くのヒトiPS細胞は，新生児表皮線維芽細胞(neonatal foreskin fibroblasts)から人工的に誘導され，“正常(non-diseased)”な指標細胞としても使用されている。しかしながら，組織を採取する段階でドナーの異常を検出できることは難しく，その匿名性からドナーの病歴の追跡は不可能である。現段階では，ヒトES/iPS細胞や分化させた細胞の病気に対する感受性を明らかにすること(どのような病気になりやすいかを予測すること)も不可能である。細胞登録の際にはドナーの病歴などに関する情報もわかっている範囲で報告すべきであるが，遺伝子の変異や欠失などの確定された情報の表記を提案している。

ヒトES/iPS細胞を培養する現場での作業

山中所長ら[4]とPollok所長ら[5]は両者とも，細胞株の名称に使用する文字数はできるだけ短くするよう主張している。データベース上で管理する際の利便性も重要だが，現場での作業も考慮するべきである。培養デッシュや凍結チューブにグローブをした手で書きやすく，読み取りやすくすることが重要である。ATCCで1.5mLチューブを用いる場合，細胞株の名称が10文字以下であることが理想的であるとPollok所長ら[5]は述べている。山中所長ら[4]も，ISCRの提案した14

表1　海外の細胞登録サイト

	機関	アドレス
Stem Cell Registry	ISCI	http://www.stem-cell-forum.net/ISCF/initiatives/isci/stem-cell-registry/
ISCR	UMass	http://www.umassmed.edu/iscr/index.aspx
hESCreg	EU連携	http://www.hescreg.eu/
NIH Human Embryonic Stem Cell Registry	NIH	http://grants.nih.gov/stem_cells/registry/current.htm

ISCI：The International Stem Cell Initiative
ISCR：The International Stem Cell Registry
UMass：The University of Massachusetts Medical School, Human Stem Cell Bank and Registry
hESCreg：European Human Embryonic Stem Cell Registry

文字[3]は不便を感じる長さであり，簡略化した名称を使用し始めるようになることを危惧する。簡略化した名称の使用は，細胞の混同のリスクにつながる。医薬基盤研JCRB細胞バンクや理化学研究所バイオリソースセンター細胞バンクでは，場合によってバーコードラベルを用いて管理している。最近は安価なバーコードリーダーもあり，研究室レベルにおいても利用が可能ではないだろうか。

これまでに命名法が規定され，広く活用されている例がある[3]。分化抗原群は，“CD42a”“CD42b”のようにCD番号で表記され，個別の抗原が認識される。また，遺伝子や蛋白質などについてはさまざまな名称が使用されるが，データベースに登録されたアクセッション番号によって識別され，容易にその原著論文まで確認できる。利便性の高い命名法の策定とデータベースの構築を行い，現場のニーズに対応する鍵となるのが，やはり細胞登録システムの整備である。細胞株の名称やIDとともに細胞情報を登録し，管理していくことが必要であろう。

ヒトES/iPS細胞の登録

ヒトES/iPS細胞を樹立した際，具体的な報告方法に関する国際的な統一規定はなく，新規の細胞の樹立を含めた研究成果の報告項目などは研究者やジャーナルの査読者に任されている。今後，産業応用される可能性があることから，各国の倫理規定を尊重して共有できるよう倫理的妥当性および科学的合理性を将来にわたって確保することが肝要である。**表1**の記載の通り，海外のヒトES細胞については，ISCBI，EUヒトES細胞登録(European Human Embryonic Stem Cell Registry：hESCreg)が連携して，それぞれのホームページで公開をしている。また，NIHヒトES細胞登録(NIH Human Embryonic Stem Cell Registry)では，NIHの研究費を使用して研究が可能な細胞が掲載されている。細胞登録に必要な情報として，**表2**に示す5つの項目が提案されている[3][8]。このようなヒトES/iPS細胞の情報整備は，新規細胞株の樹立に必要な基本データ作成とその情報公開の推進につながると思われる。

おわりに

幹細胞研究者の方々には，細胞樹立の際に前記の問題をご一考いただければ幸いである。一方で，幹細胞研究者らの声をさらに集約し，想定される問題を回避し，かつ利便性の高い命名法を早期に確立することが望まれる。ES/iPS細胞株を含む多能性幹細胞の命名法および発表に関するルールを設け，情報をデータベース化し，世界中で共有することは，幹細胞研究の推進につながる。本総説が日本の幹細胞研究推進の一助となれば幸いである。

表2　ES/iPS細胞の登録や研究成果の報告の際に必要な情報

細胞株の由来（source） 細胞のタイプ，由来組織，継代数など ドナーから採取された場合：ドナーの年齢，性別，人種（自己報告または解析結果）* 細胞バンクや民間企業から入手した場合：細胞株のアクセッション番号
樹立方法（derivation method） 細胞の株化までの方法，培地および添加物，培養期間，継代数など詳細な培養方法 ES細胞の場合：胚の取り扱い方法，胚盤胞を得るための透明帯除去方法，胚盤胞からの内部細胞塊の単離方法 iPS細胞の場合：リプログラミングに用いたベクターシステム，低分子，蛋白質，mRNAやmiRNAとその導入・誘導方法
細胞特性（characterization） 未分化状態の確認（免疫染色，フローサイトメトリー，遺伝子発現プロファイリングなど） 多能性の確認（*in vitro*分化，テラトーマ形成，遺伝子発現プロファイリングなど） 核型，SNP（一塩基多型）によるゲノム解析結果*
細胞同一確認（genetic identity）と無菌性（sterility） STR（short tandem repeat）やSNP解析による細胞認証試験結果* 無菌試験結果およびマイコプラズマ否定試験結果
細胞の来歴（provenance） ドナーに対する説明および同意（インフォームド・コンセント），利益相反についての確認

研究者から提供される細胞株の情報を名称・登録番号と合わせて管理していくべきだが，特に個人を特定できる情報（*）は，各国の倫理規定を尊重し，慎重に管理されなければならない。

謝　辞

ヒトiPS細胞研究に関与している独・医薬基盤研のすべての皆様に感謝します。なお，ヒトES，iPS細胞に関する本研究は，厚生労働省科学研究費補助金によりサポートされています。

◉文　献

1）Thomson JA, Itskovitz-Eldor J, Shapiro SS, et al : Embryonic stem cell lines derived from human blastocysts. Science **282** : 1145-1147, 1998

2）Takahashi K, Tanabe K, Ohnuki M, et al : Induction of pluripotent stem cells from adult human fibroblasts by defined factors. Cell **131** : 861-872, 2007

3）Luong MX, Auerbach J, Crook JM, et al : A call for standardized naming and reporting of human ESC and iPSC lines. Cell Stem Cell **8** : 357-359, 2011

4）Higashi H, Brüstle O, Daley G, et al : The nomenclature system should be sustainable, but also practical. Cell Stem Cell **8** : 606-607, 2011

5）Rust W, Pollok B : Reaching for consensus on a naming convention for pluripotent cells. Cell Stem Cell **8** : 607-608, 2011

6）The International Stem Cell Initiative : Characterization of human embryonic stem cell lines by the International Stem Cell Initiative. Nat Biotech **25** : 803-816, 2007

7）Narva E, Autio R, Rahkonen N, et al : High-resolution DNA analysis of human embryonic stem cell lines reveals culture-induced copy number changes and loss of heterozygosity. Nat Biotech **28** : 371-377, 2010

8）The International Stem Cell Banking Initiative : Consensus guidance for banking and supply of human embryonic stem cell lines for research purposes. Stem Cell Rev **5** : 301-314, 2009

9）Crook J, Hei D, Stacey G : The International Stem Cell Banking Initiative (ISCBI) : raising standards to bank on. In Vitro Cell Dev Biol Anim **46** : 169-172, 2010

10）Ye L, Chang JC, Lin C, et al : Induced pluripotent stem cells offer new approach to therapy in thalassemia and sickle cell anemia and option in prenatal diagnosis in genetic diseases. Proc Natl Acad Sci U S A **106** : 9826-9830, 2009.

11）Galende E, Karakikes I, Edelmann L, et al : Amniotic

fluid cells are more efficiently reprogrammed to pluripotency than adult cells. Cell Reprogram **12** : 117-125, 2010

12) Park IH, Arora N, Huo H, et al : Disease-specific induced pluripotent stem cells. Cell **134** : 877-886, 2008

13) Kazuki Y, Hiratsuka, M, Takiguchi, M, et al : Complete genetic correction of iPS cells from Duchenne muscular dystrophy. Mol Ther **18** : 386-393, 2009

14) Röehme D : Quantitative Cell Fusion : The fusion sensitivity (FS) potential. J Cell Sci **49** : 87-97, 1981

Diagnosis of bacterial endophthalmitis by broad-range quantitative PCR

Sunao Sugita,[1] Norio Shimizu,[2] Ken Watanabe,[2] Miki Katayama,[2] Shintaro Horie,[1] Manabu Ogawa,[1] Hiroshi Takase,[1] Yoshiharu Sugamoto,[1] Manabu Mochizuki[1]

[1]Department of Ophthalmology & Visual Science, Medical Research Institute, Tokyo Medical and Dental University Graduate School of Medicine and Dental Sciences, Tokyo, Japan
[2]Department of Virology, Medical Research Institute, Tokyo Medical and Dental University Graduate School of Medicine and Dental Sciences, Tokyo, Japan

Correspondence to
Dr Manabu Mochizuki, Department of Ophthalmology & Visual Science, Tokyo Medical and Dental University Graduate School of Medicine, 1-5-45 Yushima, Bunkyo-ku, Tokyo 113-8519, Japan; m.manabu.oph@tmd.ac.jp

Accepted 4 April 2010
Published Online First 31 July 2010

ABSTRACT

Aim To measure the bacterial genome in ocular fluids and to analyse the clinical relevance of infectious endophthalmitis.

Methods Nineteen ocular fluid samples (eight aqueous humour and 11 vitreous fluid samples) were collected from 19 patients with suspected bacterial endophthalmitis. Fifty ocular samples from uveitis patients were also collected along with 40 samples from patients without ocular inflammation and used as controls. Bacterial ribosomal DNA (16S rDNA) was measured by a quantitative PCR assay.

Results Bacterial 16S rDNA was detected in patients with clinically suspected bacterial endophthalmitis (18/19, 95%). With the exception of one case, high copy numbers of bacterial DNA were detected (1.7×10^3—1.7×10^9 copies/ml) in these patients. There were 10 samples (53%) with positive bacterial cultures while there were nine samples (47%) with positive Gram-staining. Real-time PCR detected bacterial 16S rDNA in three (6%) of the 50 samples from the control uveitis patients. In addition, none of the samples from the control patients without intraocular inflammation were positive.

Conclusions Quantitative broad-range PCR of bacterial 16S rDNA is a useful tool for diagnosing bacterial endophthalmitis.

INTRODUCTION

Bacterial infectious endophthalmitis occurs due to exogenous infections, such as those arising from trauma and intraocular surgery, or from endogenous infections, such as systemic infectious disorders. Previous studies have used PCR to demonstrate the presence of bacterial DNA in the ocular fluids in patients with infectious endophthalmitis.[1–10] PCR has often been used to provide evidence of bacterial involvement in the eyes with suspected intraocular infections.[8] These suspected infections include idiopathic endophthalmitis and uveitis. Recent advances in molecular biology along with the use of real-time PCR have made it possible to determine quantitative measurements of the viral load associated with viral diseases in the eye.[11–13] Several studies have recently reported finding the bacterial ribosomal RNA gene (16S rDNA) in the ocular fluids of patients with infectious endophthalmitis.[4 8 10] With primers of the bacterial 16S rRNA gene, broad-range PCR can be used to detect the presence of bacteria within the samples. In endophthalmitis patients with previous intravitreal administration of antibiotics, PCR methodology has been shown to be more effective than bacterial cultures in detecting bacterial DNA in the ocular fluids.[10] However, even broad-range PCR has not been able to determine quantitative information for the bacterial genome in the ocular sample.

In the present study, after collecting ocular samples from patients with suspected intraocular infections, which included bacterial infectious endophthalmitis, we attempted to detect and then measure the bacterial genome using real-time quantitative PCR with primers for 16S rDNA amplifications.

MATERIAL AND METHODS

Subjects

Based upon medical history and clinical observations, 69 patients with endophthalmitis and uveitis were consecutively enrolled in a prospective study that was conducted from 2008 to 2009 at the Tokyo Medical and Dental University Hospital. Samples of aqueous humour and vitreous fluids were collected from all patients. Nineteen patients (19 eyes: eight aqueous humour and 11 vitreous fluids) had bacterial infectious endophthalmitis. Of these 19 patients, six had acute postoperative endophthalmitis, four had late postoperative endophthalmitis, one had post-traumatic endophthalmitis, five had endogenous endophthalmitis, two had keratitis-associated endophthalmitis, and one had endophthalmitis after intravitreal injections of bevacizumab.

The second patient group was also a prospective study, and 50 ocular samples were collected from various patients with uveitis. The underlying pathology included idiopathic uveitis (n=21), herpetic keratouveitis (n=3), herpetic anterior iridocyclitis (n=3), acute retinal necrosis (n=5), cytomegalovirus retinitis (n=2), toxoplasmosis (n=3), toxocariasis (n=2), sarcoidosis (n=2), HTLV-1-associated uveitis (n=1), toxic lens syndrome (n=1), *Candida* endophthalmitis (n=2) and intraocular lymphoma (n=5). In this study, fungal endophthalmitis cases such as *Candida* endophthalmitis were classified as being part of this patient group. All the patients displayed active intraocular inflammation at the time of sampling.

In addition to the patient groups, we also analysed samples from a control group. These patients were enrolled in this prospective study in 2009. Forty samples (20 aqueous humour and 20 vitreous fluids) were collected from patients who did not have any type of ocular inflammation (age-related cataract, macular oedema secondary to branch retinal vein occlusion, retinal detachment, idiopathic macular hole or idiopathic epiretinal membrane).

For the ocular sampling (asepsis), the following procedures were performed in all subjects. In all of the eyes that were sampled, the ocular surfaces, including the conjunctival sacs, were rinsed once with an aqueous povidone iodine solution. Subsequently, all of these eyes were then rinsed once with a balanced-salt solution. A 0.1 ml aliquot of aqueous humour was collected aseptically in a syringe with a 30 G needle. Half of the sample was then transferred into a pre-sterilised microfuge tube and used for PCR.

In patients with endophthalmitis/uveitis who were undergoing vitreous surgery, uncontaminated non-diluted vitreous fluid samples (0.5–1.0 ml) were collected during diagnostic pars plana vitrectomy (PPV). Immediately after collection, 100 µl of the sample was transferred into a pre-sterilised microfuge tube and used for PCR. None of the asepsis samples used for analysis came from patients being given systemic antibiotics or from patients who were receiving intraocular antibiotic injections.

Conventional microbiological investigations

The Bacteria Work Station of the Tokyo Medical and Dental University Hospital processed all specimens (aqueous humour and vitreous fluids) within 1 h after the sample collection, with standard methods followed for the isolation and identification of the aerobic and anaerobic bacterial cultures. The culture methods followed conventional techniques that have been previously published.[14 15] Cultures were incubated for up to 7 days, with those lacking growth designated as culture-negative. Cytospin smears of the specimens were stained using Gram's method for detection of bacteria.

Quantitative PCR

DNA was extracted from samples using a DNA minikit (Qiagen, Valencia, California, USA) installed on a Robotic workstation for automated purification of nucleic acids (BioRobot E21, Qiagen). The real-time PCR was performed using Amplitaq Gold and the Real-Time PCR 7300 system (Applied Biosystems, Foster City, California, USA). Primers and probes of bacterial 16S rDNA and the PCR conditions are described elsewhere.[16] The sense primer (Bac349F) was 5′-AGGCAGCAGTDRGGAAT-3′ and the antisense primer (Bac806R) was 5′-GGACTACYVGGGTATCTAAT-3′. The TaqMan probe (Bac516F) was 5′-FAM-TGCCAGCAGCCGCGGTAATACRDAG-TAMRA-3′. Products were subjected to 50 cycles of PCR amplification, with cycling conditions set at 95°C for 10 min, followed by 50 cycles at 95°C for 15 s and 60°C for 1 min. Amplification of the human β-globulin gene served as an internal positive extraction and amplification control. Bacterial copy number values of more than 100 copies/ml in the sample were considered to be significant.

Sensitivity of TaqMan real-time PCR

To confirm the real-time PCR assay sensitivity, the 458 bp fragments were amplified from the DNA of *Staphylococcus aureus* (NBRC 12732) with Bac349F and Bac806R. The PCR fragments were inserted into the pGEM cloning plasmid with the pGEM T-Easy Vector Cloning System I kit (Promega, Tokyo, Japan). The plasmid was digested with restriction enzyme ScaI. Linearised plasmid was controlled by gel electrophoresis and quantified by using the Smart Ladder DNA size and mass marker (Wako, Tokyo, Japan) and the OD260 measurement. Standard curves were constructed from serial 10-fold dilutions of linearised plasmid DNA with 10 ng/µl MS2 RNA (Basel, Roche, Switzerland). The detection limit and standard range of the TaqMan real-time PCR were determined by using serial 10-fold dilutions of linearised plasmid. The standard range of DNA was linearly quantified from one to nine log DNA copies, with a detection limit of 10 copies. The negative control (nuclease-free water) was not detected.

PCR FOR 16S rRNA GENE AND SEQUENCE ANALYSIS

PCR mix (50 µl volumes) was prepared from Low-DNA AmpliTaq Gold DNA polymerase LD (Applied Biosystems). The mix comprised dATP, dGTP, dCTP, dTTP, 2 mM $MgCl_2$ and 1×Gold buffer, along with each of the primers (500 nM) (forward primer fD1-AGAGTTTGATCCTGGCTCAG; reverse primer rp2-ACGGCTACCTTGTTACGACTT).[17]

Template DNA, 1.25U of AmpliTaq Gold DNA polymerase LD (Applied Biosystems), and nuclease-free water were added to the sample. The PCR assay was performed using the Takara Thermal Cycler TP-400 (Takara Bio Inc., Shiga, Japan). The cycling conditions used were: 95°C for 10 min, followed by 35 cycles at 95°C for 15 s, 42°C for 30 s, and 72°C for 4 min. Gel electrophoresis was performed using a 0.8% agarose gel (Takara Bio Inc.) in 40 mmol/l Tris, 1 mmol/l EDTA for 30 min at 100 V, followed by ethidium bromide staining. Before cycle sequencing, amplicons were purified using the Qiaquick PCR purification kit (Qiagen) according to the manufacturer's protocol. Cycle sequencing was performed by forward and reverse priming using the Big Dye v3.1 Terminator Reaction kit (Applied Biosystems). The PCR assay was performed using a Perkin Elmer 9700 with cycling conditions set at: 95°C for 30 s, followed by 25 cycles at 96°C for 10 s, 50°C for 5 s and 60°C for 4 min. Electrophoresis was conducted in a 3130xl genetic analyser (Applied Biosystems).

We used the DNA sequence analysis to examine patients suspected of having bacterial endophthalmitis (patient samples that only had high amounts of total DNA and detected high copy numbers of bacterial 16S rDNA). Basic local alignment search tool (BLAST) analysis was used to examine the DNA sequences. The 16S rDNA sequences obtained were compared with those available in the GenBank BLAST database (http://blast.ncbi.nlm.nih.gov/Blast.cgi). Using a previously published method,[18] positive identification of the species level was defined as identification of a 16S rDNA sequence that had 99% similarity or greater with that of the GenBank BLAST strain sequence.

Prevention of bacterial contamination

To ensure that no contamination of the PCR preparation occurred, the DNA amplification and the analysis of the amplified products were done in separate laboratories. The preparation was performed on a laminar flow workbench and employed single-use aliquots of reagent and dedicated pipettes. Microfuge tubes and mineral oil aliquots were carefully sterilised prior to use.

RESULTS

Our initial PCR results indicated that bacterial 16S rDNA was positive in 18 ocular fluids of the clinically suspected bacterial endophthalmitis patients (18/19, 95%, table 1). These positive patients had high copy numbers of 16S rDNA ranging from 1.7×10^3 to 1.7×10^9 copies/ml, which indicated the presence of bacterial infection. In the one PCR-negative case (case 16 in table 1), PCR did not detect any bacterial genome in the vitreous fluid (<100 copies), although *Klebsiella pneumoniae* was detected in the biopsy sample of the liver abscess.

In the conventional bacterial cultures, 10 (53%) out of the 19 samples were positive (table 1). In addition, positive Gram staining was found in nine (47%) out of these samples. There were only two patients (cases 2 and 4 in table 1) that received

Table 1 Detection of bacterial 16S rDNA in suspected bacterial endophthalmitis and uveitis

Case	Diagnosis	Sample	Bacterial 16S rDNA	Culture	Smear	BLAST analysis	Treatment
1	Postoperative (acute)	AH	2.8×10^8 copies/ml	*Staphylococcus* spp.	Negative	nt	PPV, IAI, SA
2	Postoperative (acute)	VF	1.5×10^8 copies/ml	Negative	Negative	nt	PPV, IAI, SA
3	Postoperative (acute)	AH	1.5×10^6 copies/ml	*Staphylococcus epidermidis*	G (+)	*Staphylococcus epidermidis*	PPV, IAI, SA
4	Postoperative (acute)	VF	7.5×10^6 copies/ml	Negative	Negative	nt	PPV, IAI, SA
5	Postoperative (acute)	VF	9.0×10^7 copies/ml	Negative	G (+)	nt	PPV, IAI, SA
6	Postoperative (acute)	VF	1.9×10^7 copies/ml	*Streptococcus sanguinis*	G (+)	*Streptococcus sanguinis*	PPV, IAI, SA
7	Postoperative (late)	VF	8.1×10^7 copies/ml	Negative	Negative	*Bradyrhizobium elkanii*	PPV, IAI, SA
8	Postoperative (late)	AH	1.7×10^3 copies/ml	Negative	Negative	nt	SA
9	Postoperative (late)	AH	3.9×10^4 copies/ml	Negative	Negative	nt	SA
10	Postoperative (late)	AH	8.6×10^4 copies/ml	*Pseudomonas aeruginosa*	G (−)	nt	PPV, IAI, SA
11	Post-traumatic	VF	1.4×10^6 copies/ml	*Enterococcus faecalis*	G (+)	*Enterococcus faecalis*	PPV, SA
12	Endogenous	VF	1.3×10^7 copies/ml	*Pseudomonas* sp.	G (−)	*Pseudomonas* sp. PR	PPV, IAI, SA
13	Endogenous	VF	1.7×10^9 copies/ml	*α-Streptococcus*	G (+)	*Streptococcus mitis*	PPV, IAI, SA
14	Endogenous	AH	1.1×10^4 copies/ml	Negative	Negative	nt	IAI, SA
15	Endogenous	VF	5.5×10^6 copies/ml	*Staphylococcus aureus*	Negative	*Staphylococcus aureus*	PPV, IAI, SA
16	Endogenous	AH	<100 copies/ml	Negative	Negative	nt	PPV, IAI, SA
17	Keratitis	AH	3.1×10^6 copies/ml	*Streptococcus pneumoniae*	G (+)	*Streptococcus pneumoniae*	IAI, SA
18	Keratitis	VF	6.8×10^4 copies/ml	Negative	Negative	nt	IAI, SA
19	Intravitreal injection*	VF	1.8×10^6 copies/ml	*Streptococcus oralis*	G (+)	*Streptococcus* sp.	PPV, IAI, SA
20	Idiopathic uveitis	AH	1.4×10^3 copies/ml	Negative	nt	nt	IAI
21	Idiopathic uveitis	VF	6.1×10^4 copies/ml	Negative	Negative	nt	SA
22	CMV retinitis	AH	4.2×10^3 copies/ml	Negative	nt	nt	IAI, SA

AH, aqueous humour; BLAST, basic local alignment search tool; CMV, cytomegalovirus; IAI, intravitreal antibiotic injection; nt, not tested; PPV, pars plana vitrectomy; SA, systemic antibiotics; VF, vitreous fluids.
Using broad-range quantitative PCR, bacterial 16S rDNA could be detected in the ocular samples of the suspected bacterial endophthalmitis cases (18/19, 95%). Broad-range quantitative PCR was also used to measure the bacterial genome in the ocular samples collected from the uveitis patients (n=50) and from the three patients (6%) that were positive.
*Bacterial endophthalmitis after intravitreal injections of bevacizumab.

intravitreal injections of antibiotics prior to the PCR analysis. As shown in table 1, after examinations that included PCR, all patients received antibiotics (systemic and/or local medications).

With the exception of three out of the 50 uveitis patients, real-time PCR indicated the patients were negative for the bacterial 16S rDNA. Details for the three exceptions are shown in table 1.

The 16S rDNA was detected in two patients with idiopathic uveitis and one with cytomegalovirus (CMV) retinitis. Clinically, all of these patients were diagnosed with unilateral uveitis. Bacterial cultures were negative in all of the tested samples. In addition, bacterial 16S rDNA was not detected in any of the 40 control samples collected from the patients without ocular inflammation.

To identify the specific bacterial species, we used BLAST analysis to examine some of the bacterial infectious endophthalmitis patients. Analysis was only possible when the patient's samples had high amounts of total DNA and there was a detected high copy number of the bacterial 16S rDNA. As summarised in table 1, BLAST analysis identified *Staphylococcus epidermidis* (case 3), *Streptococcus sanguinis* (case 6), *Bradyrhizobium elkanii* (case 7), *Enterococcus faecalis* (case 11), *Pseudomonas* sp. *PR* (case 12), *Streptococcus mitis* (case 13), *Staphylococcus aureus* (case 15), *Streptococcus pneumoniae* (case 17) and *Staphylococcus* sp. (case 19). The results of the BLAST analysis were identical to the results of the bacterial culture with the exception of case 7, who was found to have a negative culture. However, even though the bacterial examinations such as bacterial cultures and smears were negative in this patient with late postoperative endophthalmitis, broad-range real-time PCR analysis of the vitreous sample yielded positive results (8.1×10^7 copies/ml). In the present study, once we were able to determine the bacterial species via the BLAST analysis and conclusively diagnose bacterial endophthalmitis, we were then able to begin treatment with antibiotics.

Case report

As seen in table 1, case 7 was a 75-year-old man who was referred to the uveitis clinic at our hospital during July 2007 due to keratic precipitates, cells and fibrin in the anterior chamber along with hypopyon and anterior vitreous opacity in his right eye (figure 1). The patient had undergone cataract surgery in his right eye 1 year prior to being seen in our clinic. Although visual acuity of his right eye at the time of his initial presentation to our clinic was 0.8, 2 months later, his visual acuity was less than 0.1. A vitreous sample was collected during the pars plana

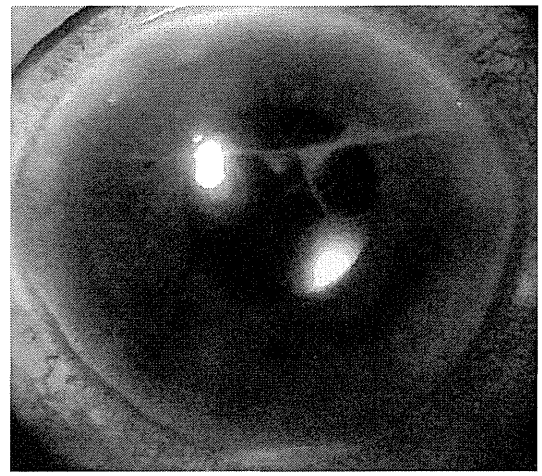

Figure 1 Case 7 (late postoperative endophthalmitis). Slit-lamp photograph in suspected bacterial endophthalmitis. In the right eye, cyclitic membrane, height of the hypopion, and severity of vitritis were seen. In this patient, broad-range quantitative PCR revealed a high copy number of the bacterial genome (8.1×10^7 copies/ml). Basic local alignment search tool (BLAST) analysis detected *Bradyrhizobium elkanii*.

vitrectomy. While bacterial culture and the Gram-staining of the vitreous sample were negative, broad-range and real-time PCR detected 8.1×10^7 copies/ml of bacterial 16S rDNA (table 1). In addition, the BLAST analysis detected *Bradyrhizobium elkanii*. After the patient was given an intravitreal antibiotic injection (vancomycin and ceftazidime) and systemic antibiotics (levofloxacin), inflammation in his right eye completely disappeared. After receiving treatment, visual acuity in his right eye recovered to 0.9 and there was no severe intraocular tissue damage noted.

DISCUSSION

In the present study, with the exception of one patient, we detected bacterial 16S rDNA in all of the cases that were clinically suspected to have bacterial endophthalmitis. In these patients, high copy numbers of the bacterial DNA were detected, which indicated the presence of a bacterial infection. In the single patient who was suspected of having infectious endophthalmitis but had no bacteria in the ocular sample, *K. pneumoniae* was detected by biopsy culture for liver infection. Thus, we were ultimately able to diagnose the patient as having endogenous endophthalmitis.

On the other hand, conventional microbiological investigations of the ocular fluid samples, such as bacterial cultures and smears, were negative in about one-half of these patients. Only three of the 50 samples collected from the patients with other clinical entities of uveitis were positive for the broad-range real-time PCR analyses of the bacterial 16S rDNA. In addition, no bacterial 16S rDNA was detected in any of the samples from the control patients without ocular inflammation.

The potential advantage of using PCR is that minute numbers of bacteria can be detected from the very small specimens that are required for the analysis. Chen *et al*[19] developed this PCR detection method for the eubacterial genome based on the conserved regions of the 16S rRNA sequence (16S rDNA) of *Escherichia coli*. As the universal primers chosen from 16S rDNA have a large amount of sequence information and highly conserved regions of the gene, primers can be synthesised for a wide variety of bacteria. In addition, the eubacterial primers used had both a high specificity and sensitivity, which was comparable to previous studies.[1 3] Hykin *et al*[1] examined 29 control vitreous samples and found four that were positive for the eubacterial genome using PCR. In a further study by Therese *et al*,[3] only a single control sample (5%) was found using the eubacterial-based PCR. In the present study, we did not detect any bacterial 16S rDNA (<100 copies/ml) in any of the samples from the control non-infectious patients when using our broad-range real-time PCR. Thus, another potential advantage of our PCR system is that it provides quantitative information for the bacterial infection. In the present study, we found false positive results (1–100 copies/ml) in only two control samples that we tested, a result that could be due to contamination caused by the conjunctival ocular flora present during the collection of the samples. Other possible causes of the contamination might be related to technical errors that occurred during the PCR preparation or perhaps due to bacterial exposure when collecting the ocular sample.

In cases of bacterial infectious endophthalmitis, it is often difficult to differentiate between inflammation caused by non-infectious and infectious agents. For example, to determine the cause of postoperative inflammation in the eye, we must consider many different possibilities, such as surgical manipulation, toxic lens syndrome, recurrent uveitis (especially if the patient has a previous history) or bacterial endophthalmitis. In the past, microbiological investigations of the ocular fluids have often failed to detect the infectious agent in bacterial endophthalmitis, resulting in a clinical dilemma regarding therapy. Deciding to use antibiotics and steroids necessitates determining whether an inflammation is infectious or sterile. Therefore, an aetiological diagnosis is essential in such cases. The use of PCR with universal eubacterial primers, which possesses broad specificities for all Gram-positive and -negative bacteria, has been recently found to be much more useful for detecting the eubacterial genome in ocular samples of postoperative endophthalmitis cases compared to the routine microbiological investigations.[2 3 5 6 8–10] In the present study, our broad-range real-time PCR for the eubacterial genome showed high correlation with the bacteriologically positive samples. This suggests that bacteriologically negative samples may include the bacterial genome. In a recent report by the French Institutional Endophthalmitis Study Groups, eubacterial PCR was found to be much more effective than bacterial cultures in detecting bacteria in vitreous samples from patients with previous intravitreal administration of antibiotics.[10] Although the previous administration of antibiotics in the PPV vitreous fluids may inhibit bacterial growth, it is assumed that PCR may still be able to detect bacterial DNA of either living or killed bacteria.

As revealed in this study, real-time PCR found only three (6%) of the 50 ocular samples from patients with unilateral uveitis to be positive. However, high copy numbers of bacterial DNA were detected in these uveitis patients, which included idiopathic uveitis (n=2) and cytomegalovirus retinitis (n=1). Endophthalmitis and uveitis positive cases with low quantification of DNA (eg, 1×10^3–1×10^4 copies/ml) cannot be differentiated according to the number of copies. Although topical or systemic steroids were administered for long periods in the idiopathic uveitis patients, the inflammation remained uncontrolled. It has also been reported that viral PCR has found cytomegalovirus DNA in the eyes of cytomegalovirus retinitis cases.[13] When these patients were given intravitreal administration of an antiviral injection (Ganciclovir), an anterior vitreous opacity was subsequently observed. There were three cases that received antibiotics (intravitreal injection and/or systemic) in our study and the intraocular inflammation, such as vitreous opacity, was well controlled by this antibiotic therapy. Although bacterial DNA amplification in such cases usually suggests contamination, antibiotic administration proved to be effective in our study. Thus, the bacterial PCR-based evidence suggests bacterial involvement in eyes that have a suspected intraocular infection. While PCR for eubacterial detection is necessary for rapid and accurate diagnosis in patients suffering from an unknown intraocular inflammatory disorder, it can also be used to accurately determine samples that are not infected. In our study we found 47 samples (94%) that had negative PCR results. Overall, our results suggest that a sensitive and rapid diagnostic test not only allows for confident verification of the diagnosis (non-infectious inflammation vs infection), but also allows for early commencement of specific and appropriate treatment. In addition, PCR analysis is able to exclude bacterial infections as the potential cause of an ocular disorder.

In conclusion, this new PCR system is an excellent diagnostic system for intraocular specimens and can be used as an alternative to further examine specimens determined to be bacteriologically negative by conventional methods. Our study also clearly demonstrated that a new diagnostic PCR system using eubacterial detection with broad-range PCR along with quantitative evaluation with real-time PCR could be extremely useful for detecting bacterial DNA within ocular samples. Recently, Goldschmidt *et al* reported that a new diagnostic test for

Propionibacteriaceae was designed using TaqMan real-time PCR.[20] Therefore, the ability to be able to collect quantitative information on bacterial infections in the eye should be useful in helping to determine clinical diagnoses and therapeutic follow-ups. Moreover, using a combination of the quantitative PCR method and the BLAST analysis to detect bacterial species is a very valuable tool for diagnosing suspected bacterial endophthalmitis. However, the DNA in 10 of 19 samples could not be sequenced using this technique and thus could not identified, which could potentially limit the clinical usefulness of this technique at the present time. In order for clinicians to be able to obtain bacterial identifications, we may need to consider additional options for the sequence analysis. In addition, in the future we will need to further verify whether this broad-range PCR can detect candidate bacterial DNA including *K. pneumoniae* in bacterial endophthalmitis.

Acknowledgements Dr Masaru Miyanaga of Miyata Hospital, and Drs Kazuichi Maruyama and Kenji Nagata of the Department of Ophthalmology, Kyoto Prefectural University of Medicine, kindly collected and sent the samples used in this study. We are very grateful for the expert technical assistance of Ms Shizu Inoue. This work was supported by Grants-in-Aid for Scientific Research (C) 20592073 and (B) 19390440 of the Ministry of Education, Culture, Sports, Science and Technology, Japan.

Competing interests None.

Patient consent Obtained.

Ethics approval This study was conducted with the approval of the Institutional Ethics Committee of Tokyo Medical and Dental University. The research followed the tenets of the Declaration of Helsinki.

Provenance and peer review Not commissioned; externally peer reviewed.

REFERENCES

1. **Hykin PG,** Tobal K, McIntyre G, *et al*. The diagnosis of delayed post-operative endophthalmitis by polymerase chain reaction of bacterial DNA in vitreous samples. *J Med Microbiol* 1994;**40**:408–15.
2. **Lohmann CP,** Heeb M, Linde HJ, *et al*. Diagnosis of infectious endophthalmitis after cataract surgery by polymerase chain reaction. *J Cataract Refract Surg* 1998;**24**:821–6.
3. **Therese KL,** Anand AR, Madhavan HN. Polymerase chain reaction in the diagnosis of bacterial endophthalmitis. *Br J Ophthalmol* 1998;**82**:1078–82.
4. **Knox CM,** Cevallos V, Margolis TP, *et al*. Identification of bacterial pathogens in patients with endophthalmitis by 16S ribosomal DNA typing. *Am J Ophthalmol* 1999;**128**:511–12.
5. **Lohmann CP,** Linde HJ, Reischl U. Improved detection of microorganisms by polymerase chain reaction in delayed endophthalmitis after cataract surgery. *Ophthalmology* 2000;**107**:1047–51.
6. **Anand AR,** Madhavan HN, Therese KL. Use of polymerase chain reaction (PCR) and DNA probe hybridization to determine the Gram reaction of the infecting bacterium in the intraocular fluids of patients with endophthalmitis. *J Infect* 2000;**41**:221–6.
7. **Okhravi N,** Adamson P, Lightman S. Use of PCR in endophthalmitis. *Ocul Immunol Inflamm* 2000;**8**:189–200.
8. **Okhravi N,** Adamson P, Carroll N, *et al*. PCR-based evidence of bacterial involvement in eyes with suspected intraocular infection. *Invest Ophthalmol Vis Sci* 2000;**41**:3474–9.
9. **Chiquet C,** Lina G, Benito Y, *et al*. Polymerase chain reaction identification in aqueous humour of patients with postoperative endophthalmitis. *J Cataract Refract Surg* 2007;**33**:635–41.
10. **Chiquet C,** Cornut PL, Benito Y, *et al*. Eubacterial PCR for bacterial detection and identification in 100 acute postcataract surgery endophthalmitis. *Invest Ophthalmol Vis Sci* 2008;**49**:1971–8.
11. **Sugita S,** Shimizu N, Kawaguchi T, *et al*. Identification of human herpes virus 6 in a patient with severe unilateral panuveitis. *Arch Ophthalmol* 2007;**125**:1426–71.
12. **Kido S,** Sugita S, Horie S, *et al*. Association of varicella zoster virus load in the aqueous humor with clinical manifestations of anterior uveitis in herpes zoster ophthalmicus and zoster sine herpete. *Br J Ophthalmol* 2008;**92**:505–8.
13. **Sugita S,** Shimizu N, Watanabe K, *et al*. Use of multiplex PCR and real-time PCR to detect human herpes virus genome in ocular fluids of patients with uveitis. *Br J Ophthalmol* 2008;**92**:928–32.
14. **Allen SD.** Anaerobic bacteria. In: Lennete Edwin H, ed. *Manual of clinical microbiology*. 4th edn. Washington DC: American Society for Microbiology, 1985:413–72.
15. **Baron EJ,** Peterson LR, Finegold SM. *Bailey and Scott's diagnostic microbiology*. 9th edn. St Louis: Mosby, 1994:79–136.
16. **Takai K,** Horikoshi K. Rapid detection and quantification of members of the archaeal community by quantitative PCR using fluorogenic probes. *Appl Environ Microbiol* 2000;**66**:5066–72.
17. **Weisburg WG,** Barns SM, Pelletier DA, *et al*. 16S ribosomal DNA amplification for phylogenetic study. *J Bacteriol* 1991;**173**:697–703.
18. **Goldenberger D,** Kunzle A. Molecular diagnosis of bacterial endocarditis by broad-range PCR amplification and direct sequencing. *J Clin Microbiol* 1997;**35**:2733–9.
19. **Chen K,** Neimark H, Rumore P, *et al*. Broad range DNA probes for detecting and amplifying eubacterial nucleic acids. *FEMS Microbiol Lett* 1989;**48**:19–24.
20. **Goldschmidt P,** Ferreira CC, Degorge S, *et al*. Rapid detection and quantification of Propionibacteriaceae. *Br J Ophthalmol* 2009;**93**:258–62.

Journal of Pathology
J Pathol 2011; **223:** 496–510
Published online 5 January 2011 in Wiley Online Library
(wileyonlinelibrary.com) DOI: 10.1002/path.2823

ORIGINAL PAPER

Activated oncogenic pathways and therapeutic targets in extranodal nasal-type NK/T cell lymphoma revealed by gene expression profiling

Siok-Bian Ng,[1]* Viknesvaran Selvarajan,[1] Gaofeng Huang,[2] Jianbiao Zhou,[3] Andrew L Feldman,[4] Mark Law,[4] Yok-Lam Kwong,[5] Norio Shimizu,[6] Yoshitoyo Kagami,[7] Katsuyuki Aozasa,[8] Manuel Salto-Tellez[1,3] and Wee-Joo Chng[2,3]*

[1] *Department of Pathology, National University Health System, Singapore*
[2] *Department of Haematology-Oncology, National University Cancer Institute of Singapore, National University Health System, Singapore*
[3] *Cancer Science Institute Singapore, National University of Singapore, Singapore*
[4] *Department of Laboratory Medicine and Pathology, Mayo Clinic, Rochester, USA*
[5] *Division of Haematology/Oncology and Bone Marrow Transplantation, Queen Mary Hospital, Hong Kong*
[6] *Department of Virology, Tokyo Medical and Dental University, Japan*
[7] *Department of Hematology, Toyota Kosei Hospital, Japan*
[8] *Department of Pathology, Osaka University Graduate School of Medicine, Japan*

**Correspondence to: Dr Siok-Bian Ng, MBBS, FRCPA, Department of Pathology, National University Hospital, 5 Lower Kent Ridge Road, Main Building, Level 3, Singapore 119074. e-mail: patnsb@nus.edu.sg*
**Correspondence to: Dr Wee-Joo Chng, MB ChB, MRCP, FRCPath, Department of Haematology–Oncology, National University Hospital, 5 Lower Kent Ridge Road, Main Building, Level 3, Singapore 119074. e-mail: mdccwj@nus.edu.sg*

Abstract

We performed comprehensive genome-wide gene expression profiling (GEP) of extranodal nasal-type natural killer/T-cell lymphoma (NKTL) using formalin-fixed, paraffin-embedded tissue ($n = 9$) and NK cell lines ($n = 5$) in comparison with normal NK cells, with the objective of understanding the oncogenic pathways involved in the pathogenesis of NKTL and to identify potential therapeutic targets. Pathway and network analysis of genes differentially expressed between NKTL and normal NK cells revealed significant enrichment for cell cycle-related genes and pathways, such as PLK1, CDK1, and Aurora-A. Furthermore, our results demonstrated a pro-proliferative and anti-apoptotic phenotype in NKTL characterized by activation of Myc and nuclear factor kappa B (NF-κB), and deregulation of p53. In corroboration with GEP findings, a significant percentage of NKTLs ($n = 33$) overexpressed c-Myc (45.4%), p53 (87.9%), and NF-κB p50 (67.7%) on immunohistochemistry using a tissue microarray containing 33 NKTL samples. Notably, overexpression of survivin was observed in 97% of cases. Based on our findings, we propose a model of NKTL pathogenesis where deregulation of p53 together with activation of Myc and NF-κB, possibly driven by EBV LMP-1, results in the cumulative up-regulation of survivin. Down-regulation of survivin with Terameprocol (EM-1421, a survivin inhibitor) results in reduced cell viability and increased apoptosis in tumour cells, suggesting that targeting survivin may be a potential novel therapeutic strategy in NKTL.

Keywords: NK/T-cell lymphoma; gene expression profiling; survivin; Myc; NF-κB; p53; paraffin-embedded tissue

Received 9 September 2010; Revised 3 November 2010; Accepted 4 November 2010

No conflicts of interest were declared.

Introduction

Extranodal nasal-type natural killer/T-cell lymphoma (NKTL) is a distinct clinicopathological entity most commonly affecting Asians and Central and South Americans, and characterized by a clonal proliferation of NK or T cells with a cytotoxic phenotype [1]. There is a strong association with Epstein–Barr virus (EBV), which manifests a type II latency pattern [2,3]. EBV is detected in the neoplastic cells in a clonal episomal form, supporting the role of the virus in tumour pathogenesis. There have been few studies investigating the oncogenic mechanisms of NKTL. These reports have identified mutations of genes regulating apoptosis, such as *FAS* and *p53*, which may contribute to the development of this tumour [4–6]. In addition, the expression of P-glycoproteins [7] and absence of granzyme B inhibitor PI9 [8] may account for the poor prognosis of patients with NKTL who were treated with chemotherapy. Like many haematolymphoid malignancies, NKTL is frequently associated with genetic alterations involving loss or gain of genetic material, the

commonest being del(6)(q21–q25) [9]. However, no specific chromosomal translocation has been identified. Iqbal *et al* [10] performed array comparative genomic hybridization on NK-cell malignancies and identified *PRDM1* as the likely target gene in del6q21. Recently, Hwang *et al* [11] performed genome-wide GEP on NKTL and identified overexpression of several genes related to vascular biology, EBV-induced genes, and platelet-derived growth factor receptor α. Deregulation of several oncogenic pathways, such as AKT, STAT3, and nuclear factor-κB pathways, was also detected. Nevertheless, comprehensive genome-wide profiling of NKTL is scarce as extensive research has been limited by the rarity of this entity, the difficulty in obtaining adequate biopsy specimens, extensive tumour necrosis, and the lack of availability of frozen tumour tissue.

Gene expression profiling (GEP) has been extensively used in cancer research in recent years. One major drawback is the requirement for frozen tissue for current methods of genome-wide expression profiling. Recently, Hoshida *et al* demonstrated the feasibility of genome-wide expression profiling of formalin-fixed, paraffin-embedded (FFPE) tissues of hepatocellular carcinoma and identified a molecular signature that correlated with survival [12]. In this study, we performed genome-wide expression profiling on a series of NKTLs using FFPE tissues in relation to normal NK cells and NK tumour cell lines, with the main objective of understanding molecular pathways deregulated in NKTL. In the process, we hope to identify potential new therapeutic targets in a disease where the outcome is poor with current treatment modalities.

Material and methods

Case selection and construction of tissue microarray

Patients with a diagnosis of NKTL were identified from the archives of the Department of Pathology, National University Hospital (NUH), from 1990 to 2009. Additional immunohistochemistry and *in situ* hybridization for EBV-encoded small RNA (EBER) were performed and the cases were classified according to the 2008 WHO lymphoma classification. Cases with no additional tissue available for immunohistochemical or genetic analysis were excluded. A total of 33 cases of NKTL were selected. According to the WHO criteria, all 33 cases expressed CD3, cytotoxic markers (granzyme B and/or TIA-1), and EBER. Immunoreactivity for CD56, CD8, and CD4 was present in 64% (21 cases), 16% (five cases), and 3% (one case), respectively. The clinical and immunophenotypic data of the cases are summarized in the Supporting information, Supplementary Table 1. Tissue microarrays (TMAs) of the 33 cases of NKTL were also constructed (see Supporting information, Supplementary methods).

Nine cases of NKTL with adequate FFPE tissue remaining and good-quality RNA were selected for GEP. In addition, two cases each of normal skin and soft tissue, intestinal, nasal, and lymph node FFPE tissue were also included for GEP analysis as control tissue. The study was approved by the Domain Specific Review Board of the National Healthcare Group, Singapore.

Immunohistochemistry (IHC)

Four-micrometre sections from the TMA blocks were cut for IHC. IHC was performed for c-Myc, p53, survivin, and five NF-κB transcription factors including p50, p52, p65, RelB, and C-Rel (see the Supporting information, Supplementary methods and Supplementary Table 2 for more details). Appropriate positive tissue controls were used.

The immunohistochemical expression for all the antibodies was scored as a percentage of the total tumour cell population per 1 mm core diameter (×400) by one of the authors (NSB). The majority of the cases (97%) had two to four cores represented on the TMA and the final score was obtained as an average of all the individual cores. For c-Myc, p53, and survivin antibodies, positive expression was defined as nuclear staining in 10% or more of the tumour population. For the five NF-κB antibodies (p50, p52, p65, RelB, and C-Rel), only nuclear immunoreactivity was regarded as constitutive NF-κB activation and positive expression was defined as nuclear staining in 10% or more of tumour cells, similar to previous published reports [13].

NK cell lines and cultures

The NK-tumour cell lines used in this study included NK-92 (American Type Culture Collection), KHYG-1 (Japanese Collection of Research Bioresources), HANK-1 (a gift from Dr Y Kagami), SNK-6, SNT-8 (a gift from Dr N Shimizu), and NK-YS (a gift from Dr YL Kwong). Culture conditions are given in the Supporting information, Supplementary methods. The phenotypic and genotypic characteristics of the NK cell lines have been well characterized in previous studies [14,15] and are summarized in the Supporting information, Supplementary Table 3.

Isolation of normal NK cells from peripheral blood

Peripheral blood mononuclear cells (PBMCs) were separated by Ficoll Paque Plus density gradient centrifugation (Amersham Biosciences, Piscataway, NJ, USA) from whole blood samples obtained from healthy donors and buffy coat packs of whole blood samples from the Blood Donation Centre, NUH. Highly pure untouched normal human NK cells were isolated using the NK cell isolation kit (Miltenyi Biotec, Bergisch Gladbach, Germany). The purity of the isolated NK cells as determined by flow cytometry was between 90% and 99%. The isolated NK cells were subsequently stimulated by culturing in the presence of human recombinant IL-2 (Miltenyi Biotec). For cell block preparation, Bouin's solution was added to the

isolated normal NK cell samples, followed by centrifugation. The packed cell sediments were fixed in formalin for tissue processing.

RNA extraction from FFPE, NK cell lines, and normal NK cells

Total RNA from NKTL FFPE tissues and FFPE normal tissue controls was isolated using a High Pure RNA Paraffin Kit (Roche Applied Science, Mannheim, Germany) according to the manufacturer's instructions. All the sections were deparaffinized with xylene, subjected to proteinase K digestion, and RNA was extracted according to the manufacturer's protocol.

Total RNA was extracted from freshly isolated cells from NK cell lines and normal NK cell samples obtained from healthy donors using the miRNeasy Mini Kit (Qiagen GmbH, Hilden, Germany) protocol with DNaseI treatment included. The concentration and purity of the total RNA extracted were measured using a NanoDrop ND 3.0 spectrophotometer (NanoDrop Technologies Inc, Wilmington, DE, USA). RNA quality was assessed with an Agilent 2100 Bioanalyzer (Agilent Technologies, Palo Alto, CA, USA) and an RNA 6000 LabChip Kit (Agilent Technologies). Of the samples with RNA extracted, nine met the quality requirements and were used for GEP and subsequent analysis.

Gene expression profiling and analysis

GEP was performed according to the complementary DNA-mediated annealing, selection, extension, and ligation (DASL) assay (Illumina, Inc, San Diego, CA, USA) [16,17]. Raw signal intensities of each probe were obtained from data analysis software (Beadstudio; Illumina, San Diego, CA, USA). The data were normalized using a linear calibration method. Hierarchical clustering of samples was performed using the Pearson coefficient and the Ward method as the similarity and linkage methods, respectively, using the Bioconductor packages of R. To derive the NKTL-specific gene expression profiles, we extracted genes differentially expressed between NK cell lines and NKTL FFPE samples, and normal NK cells and normal FFPE controls using significance analysis of microarray (SAM) [18] (see Supporting information, Supplementary methods).

To further understand the functional and biological relevance of differentially expressed genes, gene ontology and pathway/network analysis was performed using the web-based software MetaCore (GeneGo, St Joseph, MI, USA). The software contains an interactive, manually annotated database derived from literature publications on proteins and small molecules that allows for representation of biological functionality and integration of functional, molecular, and clinical information. Several algorithms to enable both the construction and the analysis of gene networks were integrated as previously described [19]. The output p values reflect scoring, prioritization, and statistical significance of networks according to the relevance of input data.

Quantitative PCR for validation of selected genes

A reverse transcription reaction was carried out using the High Capacity cDNA Reverse Transcription Kit system (ABI, Foster City, CA, USA). Real-time fluorescent monitoring of the PCR products was performed using the Power SYBR Green PCR Master Mix (ABI) and gene-specific primers (Supporting information, Supplementary Table 4). Real-time PCR was performed in the ABI PRISM 7300 Sequence Detection system (Applied Biosystems, foster city, CA, USA) and analysed utilizing Sequence Detection Software v1.4 (ABI). Using endogenous GAPDH as an internal control for comparison, relative quantification of gene expression levels was performed and calculated using $2(-\Delta\Delta CT)$.

FISH for c-Myc translocation

MYC breakapart (BAP) probes were designed using the University of California Santa Cruz Genome Browser (http://www.genome.UCSC.edu) to identify bacterial artificial chromosomes (BACs) flanking the genes of interest (Supporting information, Supplementary Table 5). DNA was isolated (Plasmid Maxi Kit; Qiagen, Valencia, CA, USA) from BAC clones (ResGen™; Invitrogen, Carlsbad, CA, USA) and labelled with Texas Red-dUTP (Molecular Probes, Invitrogen, Carlsbad, CA, USA) or SpectrumGreen-dUTP (Abbott Molecular, Des Plaines, IL, USA). FISH was performed on TMA sections and scored as previously described [20]. Sections were analysed qualitatively by a microscopist (ML) and a minimum of 50 cells with strong FISH signals was required for a sample to be considered informative.

Terameprocol (EM-1421) treatment of NK cell lines

NK cell lines were treated with varying concentrations of the BIRC5 inhibitor Terameprocol (EM-1421; Erimos Pharmaceuticals, Houston, TX, USA) [21, 22] and control. Following incubation for 48 h, the cells were harvested, washed in PBS, and subjected to (i) MTS assay to evaluate the degree of cell viability (see Supporting information, Supplementary methods); (ii) flow cytometric analysis to assess the degree of apoptotic cell death using Annexin-V-APC and propidium iodide (PI) staining (BD Pharmigen, CA, USA); and (iii) western blot analysis to confirm successful inhibition of BIRC5 (Supporting information, Supplementary methods). The flow cytometry analysis was performed on a BD LSR II flow cytometer (Becton Dickinson, CA, USA) using BD FACSDiva™ software.

Table 1. Pathways and cellular processes enriched in genes differentially expressed between NKTL and normal NK cells

Map	Map folders	Cell process	*p* value	Objects in gene list	Objects in map
Cell cycle_The metaphase checkpoint	Congenital, Hereditary, and Neonatal Diseases and Abnormalities Regulatory processes/Cell cycle	Cell cycle	4.01E-05	10	36
Cell cycle_Chromosome condensation in prometaphase	Regulatory processes/Cell cycle	Cell cycle	1.21E-04	7	20
Cell cycle_Transition and termination of DNA replication	Regulatory processes/Cell cycle	Cell cycle	7.48E-04	7	26
Cell cycle_Start of DNA replication in early S phase	Regulatory processes/Cell cycle	Cell cycle	2.30E-03	7	31
Cell cycle_Role of APC in cell cycle regulation	Regulatory processes/Cell cycle	Cell cycle	2.79E-03	7	32
Cell cycle_Initiation of mitosis	Congenital, Hereditary, and Neonatal Diseases and Abnormalities Regulatory processes/Cell cycle	Cell cycle	3.42E-03	6	25
Cell cycle_Spindle assembly and chromosome separation	Regulatory processes/Cell cycle	Cell cycle	1.22E-02	6	32
DNA damage_ATM/ATR regulation of G2/M checkpoint	Congenital, Hereditary, and Neonatal Diseases and Abnormalities Regulatory processes/Cell cycle Regulatory processes/DNA damage	Cell cycle	1.96E-02	5	26
Transcription_Sin3 and NuRD in transcription regulation	Regulatory processes/Transcription	Transcription	2.73E-02	6	38
Cell cycle_Cell cycle (generic schema)	Congenital, Hereditary, and Neonatal Diseases and Abnormalities Regulatory processes/Cell cycle	Cell cycle	3.72E-02	4	21
Development_MAG-dependent inhibition of neurite outgrowth	Congenital, Hereditary, and Neonatal Diseases and Abnormalities Protein function/Growth factors Regulatory processes/Development/Neurogenesis	Intracellular receptor-mediated signalling pathway, response to extracellular stimulus	4.44E-02	5	32

Results

Analysis of GEP of NKTL

We compared the gene expression of NKTL FFPE samples ($n = 9$) with that of normal NK cells, as well as the respective normal FFPE tissue controls from nasal, skin and soft tissue, intestinal tract, and lymph node (see Supporting information, Supplementary methods). Among the genes showing at least a two-fold and statistically significant difference ($p < 0.05$), 339 were found to be up-regulated and 737 were down-regulated in NKTL compared with normal NK cells (Supporting information, Supplementary Table 6). We performed quantitative PCR validation on a few interesting genes frequently involved in tumour oncogenesis, including *BIRC5* (*survivin*), *EZH2*, *STMN1*, and *WHSC1*. On the whole, the quantitative PCR results were consistent with GEP data showing overexpression of *BIRC5*, *EZH2*, and *STMN1* in NK cell lines compared with normal NK cells (see the Supporting information, Supplementary Figure 1).

These differentially expressed genes were significantly enriched for cell cycle-related pathways and processes (Table 1), suggesting that NKTLs are significantly more proliferative than normal NK cells. Amongst the key proteins involved in cell cycle and mitosis are PLK1, CDK1, and Aurora-A. These proteins may also be potential therapeutic targets because of their involvement in carcinogenesis [23–25].

Using MetaCore, we found that the differentially expressed genes between NKTL and normal NK cells were enriched for targets of a number of transcription factors including Myc, p53, and NF-κB subunits (Table 2). When we further examined the expression of the Myc transcription targets and their relationship with Myc, it was striking that most of the genes up-regulated and down-regulated in our list of differentially expressed genes have been shown by previous experiments to be concordantly expressed and repressed by Myc (Figure 1A). This result suggests that Myc is activated in NKTL compared with normal NK cells. In contrast, the transcription targets of p53 in our list of differentially expressed genes showed a predominantly opposite effect to what is expected under normal p53 control, ie genes that are normally repressed by p53 were up-regulated in NKTL compared with normal NK cells, and vice versa (Figure 1B), indicating deregulation of the p53 transcription factor in NKTL compared with normal NK cells.

We further assessed the expression of a previously published NF-κB signature [26] and a validated MYC signature (unpublished) in the gene expression dataset.

Table 2. Targets of transcription targets enriched amongst genes differentially expressed between NKTL and normal NK cells

No	Network	GO processes	Total nodes	Root nodes	*p* value	zScore	gScore
1	c-Myc	Cell cycle (33.8%; 4.867e-13), cell division (21.1%; 2.325e-12), cell cycle process (26.8%; 4.968e-11), cell cycle phase (23.9%; 5.019e-11), mitotic cell cycle (21.1%; 5.843e-10)	73	72	3.28E-149	89.37	89.37
2	SP1	Cell division (13.8%; 2.728e-06), positive regulation of cellular process (35.4%; 3.296e-06), positive regulation of catalytic activity (18.5%; 4.041e-06), regulation of catalytic activity (23.1%; 4.731e-06), regulation of molecular function (24.6%; 4.773e-06)	65	64	2.66E-132	84.18	84.18
3	p53	Regulation of cell cycle (26.7%; 3.272e-11), cell cycle (33.3%; 5.758e-11), cell division (20.0%; 7.506e-10), cell cycle process (26.7%; 1.779e-09), cell cycle checkpoint (13.3%; 2.766e-09)	62	61	5.59E-126	82.15	82.15
4	ESR1 (nuclear)	Regulation of cell cycle (25.0%; 2.165e-08), cell division (18.8%; 1.881e-07), cell cycle checkpoint (12.5%; 4.328e-07), regulation of mitotic cell cycle (14.6%; 6.202e-07), negative regulation of cellular process (39.6%; 1.318e-06)	53	52	4.48E-107	75.73	75.73
5	CREB1	Cell cycle (31.7%; 2.639e-07), M phase (22.0%; 3.244e-07), regulation of cell cycle (24.4%; 4.238e-07), cell division (19.5%; 6.635e-07), cell cycle phase (22.0%; 4.111e-06)	42	41	4.25E-84	67.07	67.07
6	RelA (p65 NF-κB subunit)	Regulation of cell proliferation (38.9%; 2.214e-08), positive regulation of biological process (52.8%; 6.173e-08), developmental process (69.4%; 8.591e-08), biological regulation (94.4%; 8.778e-08), positive regulation of cellular process (50.0%; 8.804e-08)	38	37	8.86E-76	63.63	63.63
7	GATA-1	Cell division (22.9%; 1.798e-07), regulation of cell cycle (25.7%; 9.966e-07), M phase (22.9%; 1.068e-06), cell cycle checkpoint (14.3%; 2.108e-06), cell cycle (31.4%; 2.446e-06)	35	34	1.49E-69	60.92	60.92
8	Androgen receptor	Regulation of cell cycle (33.3%; 1.553e-08), M phase (30.0%; 1.661e-08), cell cycle (40.0%; 3.930e-08), cell division (26.7%; 4.844e-08), negative regulation of cellular process (53.3%; 5.874e-08)	33	32	2.07E-65	59.04	59.04
9	c-Fos	Biological regulation (93.8%; 8.492e-07), regulation of metabolic process (62.5%; 2.756e-06), regulation of cellular process (87.5%; 4.280e-06), regulation of cell cycle (25.0%; 5.084e-06), M phase (21.9%; 7.025e-06)	32	31	2.44E-63	58.09	58.09
10	c-Rel (NF-κB subunit)	Regulation of cell cycle (31.0%; 1.674e-07), cell cycle (34.5%; 2.717e-06), M phase (24.1%; 3.459e-06), mitotic cell cycle (24.1%; 9.697e-06), cell division (20.7%; 1.212e-05)	31	30	2.85E-61	57.11	57.11
11	HNF6	Regulation of cell cycle (31.0%; 1.674e-07), M phase (27.6%; 2.200e-07), cell cycle (37.9%; 2.788e-07), cell division (24.1%; 7.233e-07), mitotic cell cycle (27.6%; 7.253e-07)	30	29	3.33E-59	56.12	56.12
12	PPAR-gamma	Regulation of cell cycle (31.0%; 1.674e-07), cell cycle (37.9%; 2.788e-07), cell division (24.1%; 7.233e-07), mitotic cell cycle (27.6%; 7.253e-07), cell cycle checkpoint (17.2%; 7.936e-07)	29	28	3.87E-57	55.11	55.11
13	STAT3	M phase (27.6%; 2.200e-07), cell cycle (37.9%; 2.788e-07), cell division (24.1%; 7.233e-07), mitotic cell cycle (27.6%; 7.253e-07), cell cycle process (31.0%; 1.649e-06)	29	28	3.87E-57	55.11	55.11
14	E2F1	Cell division (42.9%; 2.758e-14), cell cycle (57.1%; 1.936e-13), mitotic cell cycle (42.9%; 2.870e-12), cell cycle phase (42.9%; 1.646e-11), DNA metabolic process (42.9%; 3.985e-11)	28	27	4.49E-55	54.08	54.08
15	HIF1A	Regulation of cell cycle (37.0%; 4.751e-09), negative regulation of cellular process (55.6%; 7.431e-08), cell cycle (40.7%; 1.168e-07), negative regulation of biological process (55.6%; 2.183e-07), regulation of mitotic cell cycle (22.2%; 2.953e-07)	27	26	5.19E-53	53.03	53.03
16	CDP/Cux	Cell cycle (59.3%; 8.763e-14), M phase (37.0%; 2.405e-10), mitotic cell cycle (37.0%; 1.107e-09), mitosis (29.6%; 2.891e-09), M phase of mitotic cell cycle (29.6%; 3.407e-09)	27	26	5.19E-53	53.03	53.03

Table 2. (*Continued*)

No	Network	GO processes	Total nodes	Root nodes	*p* value	zScore	gScore
17	N-Myc	Cell cycle (46.2%; 5.436e-09), cell division (30.8%; 1.378e-08), regulation of cell cycle (34.6%; 5.685e-08), mitotic cell cycle (30.8%; 2.836e-07), cell cycle checkpoint (19.2%; 4.460e-07)	26	25	5.97E-51	51.96	51.96
18	GCR-alpha	Negative regulation of cellular process (57.7%; 3.722e-08), negative regulation of biological process (57.7%; 1.105e-07), cell division (26.9%; 3.196e-07), cell cycle (38.5%; 8.437e-07), regulation of cell cycle (30.8%; 8.926e-07)	26	25	5.97E-51	51.96	51.96
19	AML1 (RUNX1)	Regulation of cell cycle (38.5%; 3.078e-09), cell cycle (46.2%; 5.436e-09), cell division (30.8%; 1.378e-08), mitotic cell cycle (34.6%; 1.544e-08), cell cycle process (38.5%; 4.140e-08)	26	25	5.97E-51	51.96	51.96
20	TCF7L2 (TCF4)	Negative regulation of cellular process (60.0%; 1.775e-08), regulation of cell cycle (36.0%; 3.824e-08), cell cycle (44.0%; 4.443e-08), negative regulation of biological process (60.0%; 5.327e-08), cell cycle process (36.0%; 3.906e-07)	25	24	6.85E-49	50.87	50.87
21	VDR	Cell division (28.0%; 2.373e-07), cell cycle (40.0%; 5.473e-07), regulation of cell cycle (32.0%; 6.354e-07), M phase (28.0%; 1.154e-06), mitotic cell cycle (28.0%; 3.281e-06)	25	24	6.85E-49	50.87	50.87
22	ATF-2	Cell cycle (40.0%; 5.473e-07), regulation of cell cycle (32.0%; 6.354e-07), M phase (28.0%; 1.154e-06), mitotic cell cycle (28.0%; 3.281e-06), cell division (24.0%; 4.806e-06)	25	24	6.85E-49	50.87	50.87
23	IRF1	Regulation of cell cycle (36.0%; 3.824e-08), cell cycle (40.0%; 5.473e-07), M phase (28.0%; 1.154e-06), mitotic cell cycle (28.0%; 3.281e-06), cell division (24.0%; 4.806e-06)	25	24	6.85E-49	50.87	50.87
24	FKHR	Cell cycle (41.7%; 3.461e-07), regulation of cell cycle (33.3%; 4.443e-07), negative regulation of cellular process (54.2%; 8.335e-07), M phase (29.2%; 8.479e-07), post-translational protein modification (45.8%; 1.468e-06)	24	23	7.83E-47	49.75	49.75
25	Brca1	Regulation of cell cycle (41.7%; 1.203e-09), cell cycle (50.0%; 1.694e-09), cell cycle checkpoint (25.0%; 5.340e-09), cell cycle process (41.7%; 1.649e-08), mitotic cell cycle (33.3%; 1.401e-07)	24	23	7.83E-47	49.75	49.75
26	RARalpha	Cell division (29.2%; 1.736e-07), cell cycle (41.7%; 3.461e-07), regulation of cell cycle (33.3%; 4.443e-07), negative regulation of cellular process (54.2%; 8.335e-07), M phase (29.2%; 8.479e-07)	24	23	7.83E-47	49.75	49.75
27	MYOD	Cell cycle (41.7%; 3.461e-07), regulation of cell cycle (33.3%; 4.443e-07), M phase (29.2%; 8.479e-07), cell differentiation (54.2%; 1.202e-06), post-translational protein modification (45.8%; 1.468e-06)	24	23	7.83E-47	49.75	49.75
28	HMGI/Y	Cell cycle (43.5%; 2.128e-07), regulation of cell cycle (34.8%; 3.046e-07), M phase (30.4%; 6.128e-07), mitotic cell cycle (30.4%; 1.754e-06), cell cycle process (34.8%; 2.387e-06)	23	22	8.91E-45	48.61	48.61
29	HOXD13	Cell division (30.4%; 1.249e-07), cell cycle (43.5%; 2.128e-07), regulation of cell cycle (34.8%; 3.046e-07), M phase (30.4%; 6.128e-07), regulation of cell proliferation (43.5%; 6.871e-07)	23	22	8.91E-45	48.61	48.61
30	PPARGC1 (PGC1-alpha)	Cell cycle (43.5%; 2.128e-07), regulation of cell cycle (34.8%; 3.046e-07), M phase (30.4%; 6.128e-07), mitotic cell cycle (30.4%; 1.754e-06), cellular biopolymer metabolic process (87.0%; 1.992e-06)	23	22	8.91E-45	48.61	48.61

Consistent with the MetaCore analysis, we observed that the MYC and NF-κB signatures were highly expressed in the NK cell lines and tumour samples compared with normal NK cells. When these two signatures were summarized into indices using the median expression of genes constituting the respective signatures, both the NF-κB index and the MYC index were significantly higher in NK cell lines and NKTL than in normal NK cells (Figure 1C).

As NKTL is an aggressive lymphoma often with extranodal involvement, we wanted to see if there was any enrichment among dysregulated genes for cell

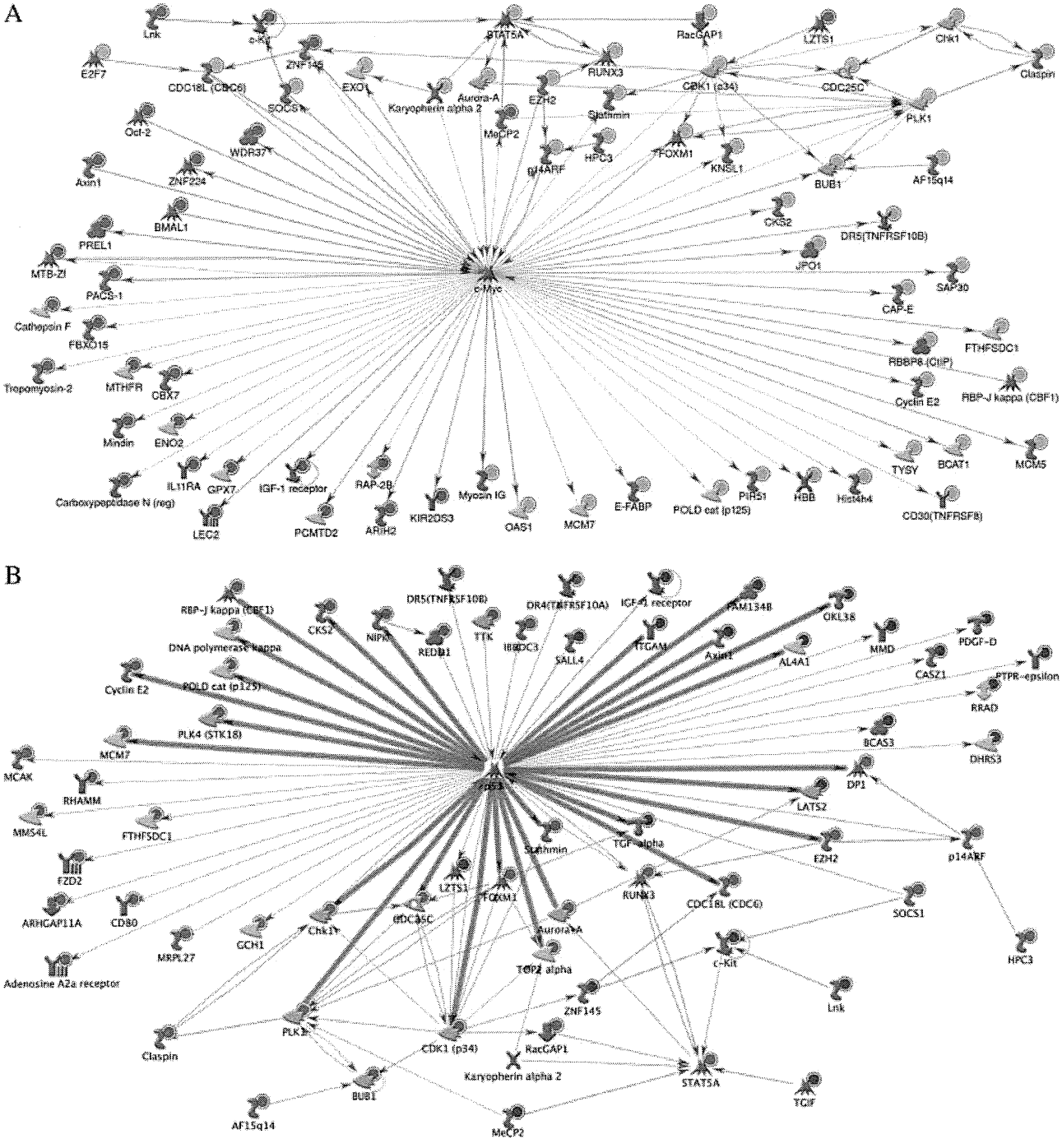

Figure 1. Gene expression profiling and networks formed by genes differentially expressed between NKTL and normal NK cells as analysed using MetaCore. (A) Network comprising transcriptional targets of MYC. Most of the transcriptional targets are expressed in concordance with the expected effect of MYC activation. (B) On the other hand, expression of transcriptional targets of p53 is discordant with the expected effect of p53 activated (interactions highlighted by magenta colour). In these figures, genes in our differentially expressed gene list (Supporting information, Supplementary Table 6) are indicated by a red circular 'target' or a blue circular 'target' to the upper right of the gene symbols if overexpressed or underexpressed, respectively. The directions of arrows connecting different molecules indicate the direction of interaction. Connecting lines in green represent a stimulating interaction and those in red an inhibitory interaction. If the line is in grey, the nature of the interaction is unknown. The different symbols signify different functions of each molecule, eg transcription factors, receptors, etc. (C) Heat map showing expression of NF-κB and MYC signatures in NK cell lines, NKTL and normal NK cells, and tissue control. Overexpressed and underexpressed genes are in red and green, respectively, with yellow indicating median expression. The dot-plot indicates that when these signatures are summarized into indices, both the NFKB and the MYC indices are significantly higher in NK cell lines and NKTL than in normal NK cells.

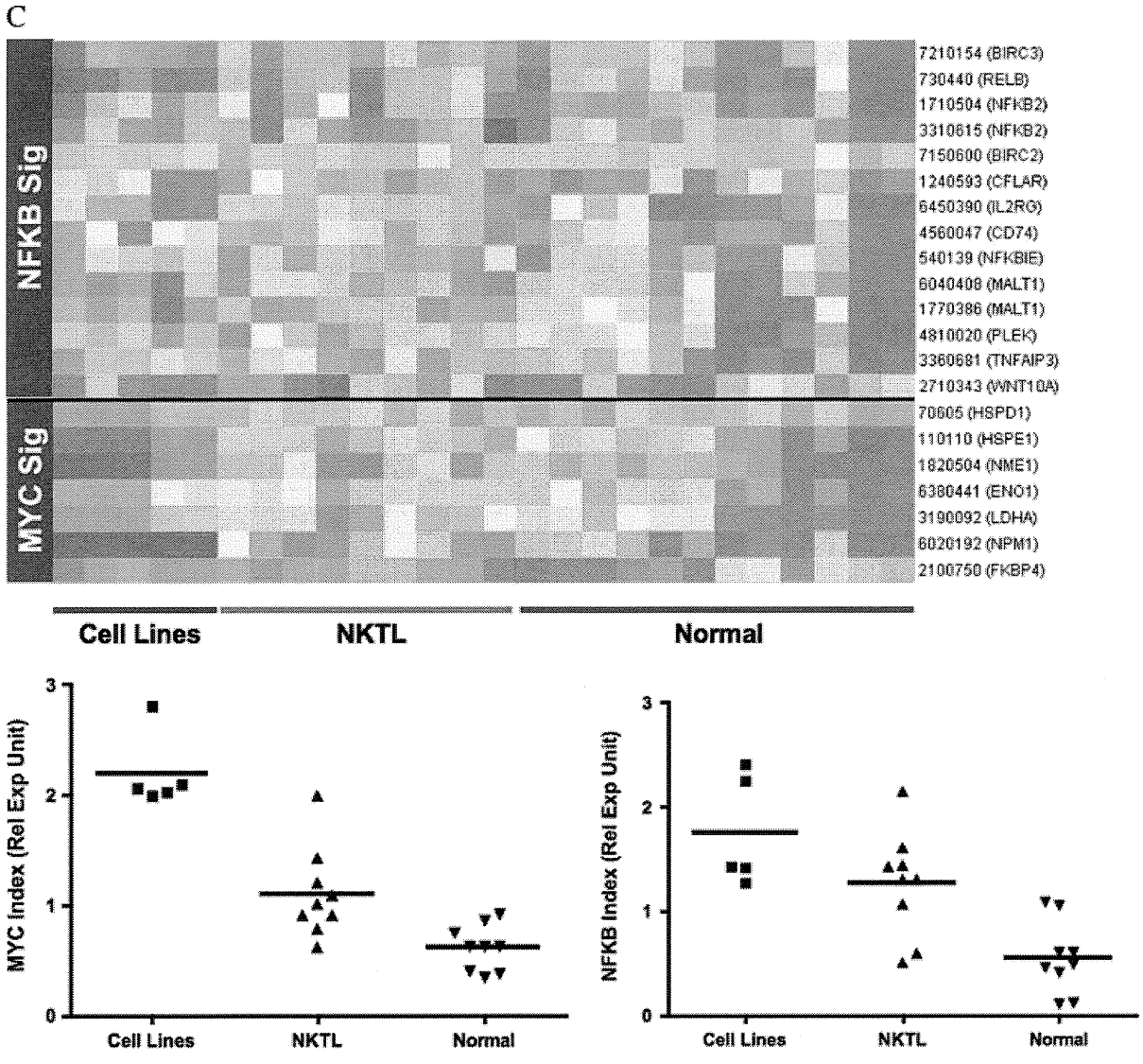

Figure 1. (*Continued*).

adhesion or metastasis-related genes. We performed Individual Pathway Activity Score Analysis (iPASA, http://lab.selfip.net/iPASA/) [27], a modification of gene set enrichment analysis, and found several metastasis-related gene sets to have higher scores in NKTL and NK cell lines than in normal NK cells (Supporting information, Supplementary Figure 2). However, an analysis of the genes contributing most significantly to the high scores of these gene sets suggested that this was predominantly due to cell cycle-related genes (Supporting information, Supplementary Figure 3).

Immunohistochemistry

To validate our gene expression results, we performed IHC for c-Myc, p53, all five subunits of the NF-κB pathway, and survivin on TMA sections containing 33 samples of NKTL. In corroboration with the GEP findings, we observed a significant percentage of our NKTL cases showing positive expression for c-Myc (15/33, 45.4%), p53 (29/33, 87.9%), NF-κB p50 (21/31, 67.7%), and survivin (32/33, 97%) (Figure 2 and Supporting information, Supplementary Table 7). Furthermore, there was a significant correlation between c-Myc immunoreactivity and the

Figure 2. Validation of gene expression profiling by IHC. (A, B) Case NKTL 23 showing nuclear expression of c-Myc in the medium and large tumour cells. (A) H&E (B) c-Myc. (C, D) Case NKTL 33 showing strong p53 nuclear staining in the neoplastic cells, which range from small to large and display irregular nuclear contours. (C) H&E (D) p53. (E, F) Strong nuclear expression for survivin observed in the medium and large neoplastic lymphocytes in case NKTL 32. (E) H&E (F) survivin. (G, H) Case NKTL 9 with positive nuclear and cytoplasmic staining for p50 in the small neoplastic lymphocytes. Only nuclear expression is regarded as constitutive p50 activation. (G) H&E (H) p50. (I, J) Moderate to strong nuclear and cytoplasmic immunoreactivity for RelB in the large pleomorphic lymphoid cells of case NKTL 6. (I) H&E (J) RelB. All photographs were taken with a DP20 Olympus camera (Olympus, Tokyo, Japan) using an Olympus BX41 microscope (Olympus). Images were acquired using DP Controller 2002 (Olympus) and processed using Adobe Photoshop version 5.5 (Adobe Systems, San Jose, CA, USA). Original magnifications: ×600 (A–J).

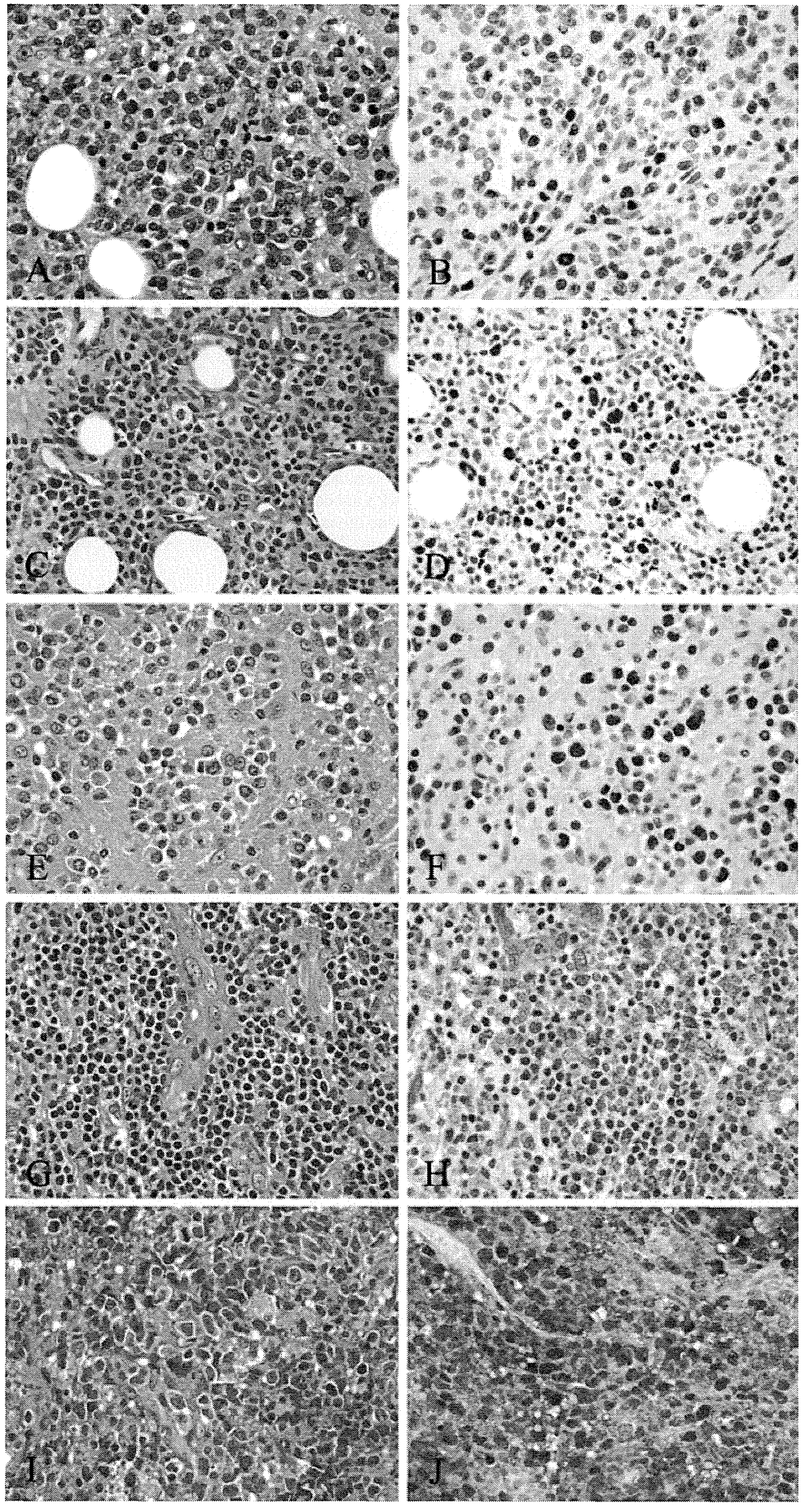

Figure 2.

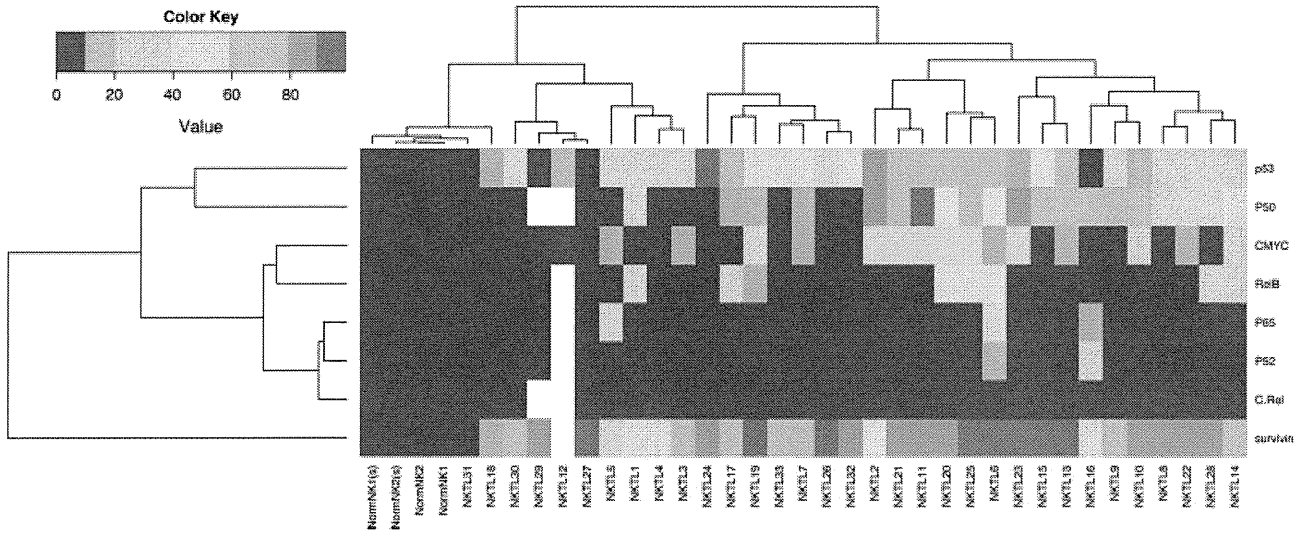

Figure 3. Clustering of samples based on expression of markers on IHC in NKTL (heat map). The samples used for IHC analysis were clustered based on the percentage of cells expressing the different markers used for IHC. Almost all cases of NKTL expressed aberrant p53 and survivin (not expressed in normal NK cells). Two main groups of NKTLs are defined by the expression pattern of these markers, with one group having c-Myc expression and stronger p50 expression, whereas the other only occasionally expresses c-Myc and p50. The legend for the colour coding in the heat map is shown to the upper left of the figure. 'White' indicates that tissue was not available for IHC staining of these markers.

MYC index (Supporting information, Supplementary Figure 4). Using FISH analysis, no break-apart signals were observed in 12 cases with adequate tumour cells and adequate hybridization, suggesting that MYC activation is not due to MYC rearrangements. In addition to p50, which is involved in the canonical NF-κB pathway, 27.3% (9 of 33) of NKTLs demonstrated positive expression for RelB, indicating that the non-canonical pathway may also be activated in a subset of NKTLs. In contrast, p52 and p65 were only infrequently expressed in 2 of 32 and 3 of 32 cases, respectively. None of our cases expressed c-Rel. Particularly striking was the immunoreactivity for survivin, where 29 out of the 32 positive cases (91%) showed expression in 50% or more of the tumour cell population, with strong staining in the majority of the cases. As expected, normal NK cells showed no expression or less than 10% expression for all the antibodies (Supporting information, Supplementary Table 8).

In order to study the relationship between the activation of Myc, p53, and NF-κB pathways and to determine whether there are distinct clusters based on the combination of these pathways, we clustered the samples according to the level of immunoreactivity for the different antigens (Figure 3). Almost all samples overexpressed p53 and survivin. Two main clusters were observed. The first, with hardly any expression of the markers tested, was clustered together with the normal NK cell samples. The second large cluster contained the remaining samples, with aberrant expression of one or more of these markers. Within the second cluster were two sub-clusters, one showing higher expression of p50 and c-Myc compared with the other. The clinical relevance of the different patterns of expression of these markers is not known as our sample size was small and there was no apparent difference in survival between these groups when we correlated the data with clinical outcome (data not shown).

Inhibition of survivin leads to apoptosis in NKTL cell lines

As survivin was aberrantly expressed in most of the NKTLs, we investigated whether inhibition of survivin would be therapeutically useful. We used western blot to assess the level of survivin protein expression in five NK cell lines (KHYG-1, NK-92, NK-YS, HANK-1, and SNK-6) and found overexpression of survivin in NK cell lines compared with normal NK cells, consistent with the IHC results (Figure 4A). The three cell lines with the highest survivin expression (KHYG-1, NK-92, and SNK-6) were selected for treatment with Terameprocol (EM-1421), a survivin inhibitor [21,22]. Successful suppression of survivin confirmed by western blot (Figure 4B) in KHYG-1 and NK92 resulted in a significant decrease in cell viability using the MTS assay (Figure 4C) and a dose-dependent increase in apoptosis compared with the control, as demonstrated in the bar chart (Figure 4D). In contrast, no significant change in cell viability or apoptosis in SNK-6 was observed when survivin was not suppressed by the inhibitor.

Discussion

NKTL is a relatively rare lymphoma that is highly aggressive, and current treatment strategies are clearly sub-optimal and chemoresistance is common [8,28]. A better understanding of the molecular abnormalities underlying this condition will provide important insights into the biology of this disease. In the past,

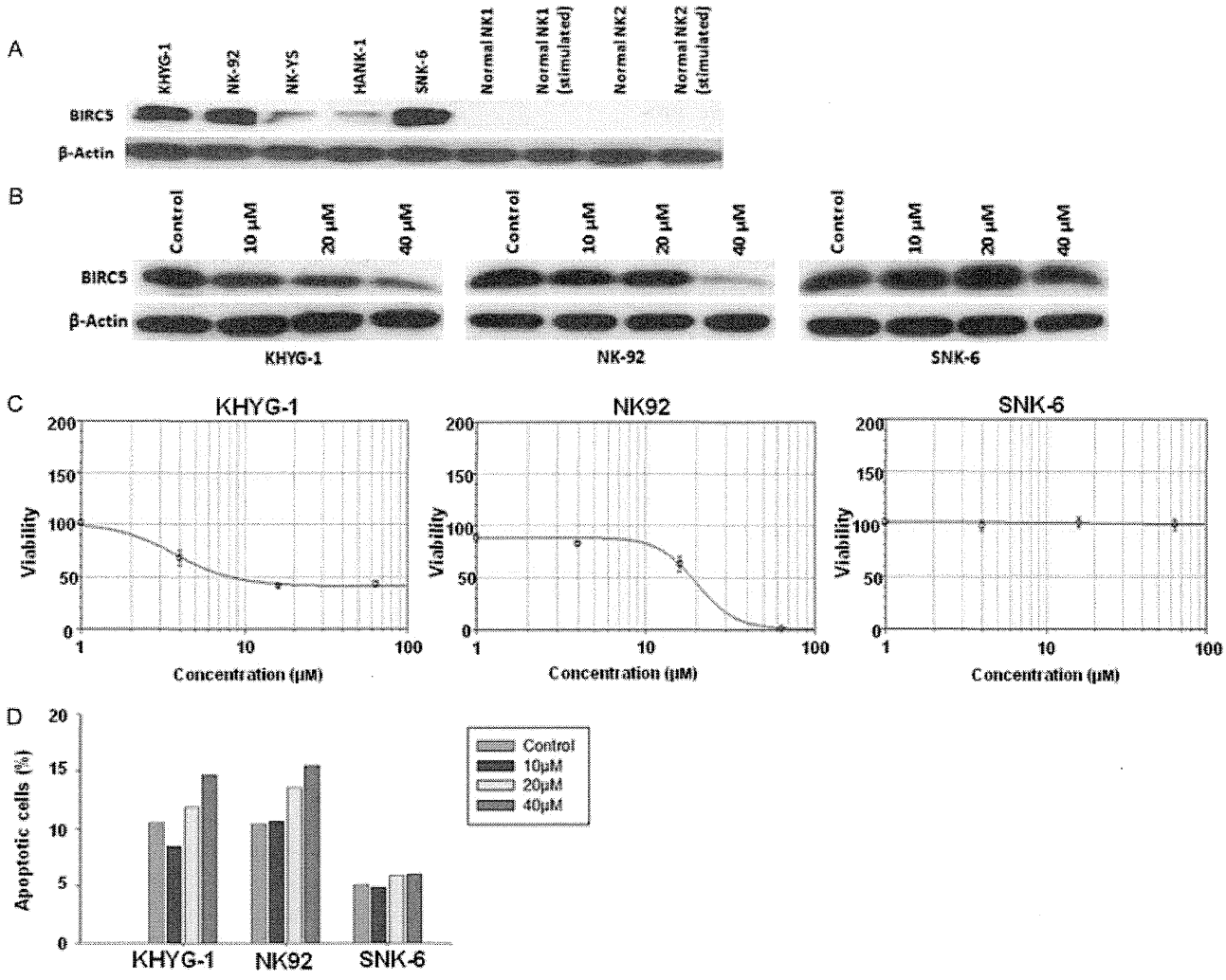

Figure 4. Inhibition of survivin leads to apoptosis in NK cell lines. Three NK cell lines with high expression of survivin (KHYG-1, NK-92, and SNK-6) identified by western blot (A) were treated with Terameprocol (survivin inhibitor) at 10, 20, and 40 μM or control for 48 h. There was successful dose-dependent inhibition of survivin in KHYG-1 and NK-92, confirmed by western blot with β-actin as the loading control (B). This was accompanied by a decrease in more than 50% of cell viability in the two cell lines and an increase in apoptosis detected by flow cytometry (C, D). The different concentrations of Terameprocol are represented by different colours according to the colour legend on the upper right of figure D. In contrast, there was no significant increase in apoptosis or decrease in cell viability in SNK-6 when survivin was not suppressed by the inhibitor.

it has been impossible to perform GEP using FFPE, due to RNA fragmentation. However, recent technology has enabled good-quality gene expression data to be obtained from FFPE samples [12]. We have shown in our study using a similar platform that we can obtain useful and meaningful GEP results from FFPE tissue. The validity of our results was supported by quantitative PCR validation as well as corroboration of our in silico functional analysis with immunohistochemistry in a larger TMA dataset, showing a good correlation between GEP, IHC, and western blot results. We did not attempt to categorize our cases into different clinical subtypes according to the site of involvement or cell of origin because of the small sample size.

Our results demonstrate a pro-proliferative and anti-apoptotic phenotype in NKTL, compared with normal NK cells, which is characterized by the activation of Myc and NF-κB, and deregulation of p53. NF-κB transcription factors are key regulators of immune, inflammatory, and acute phase responses [29] that have been implicated in oncogenesis through their transcription regulation of genes involved in cell cycle proliferation and cell adhesion, inhibition of apoptosis (including survivin) [30], and induction of cancer treatment resistance via the expression of multi-drug resistance-1 in tumour cells [30]. Among lymphoid malignancies, activation of NF-κB has been reported in mycosis fungoides [31], classical Hodgkin lymphoma, anaplastic large cell lymphoma, and peripheral T-cell lymphoma [32]. In NKTL, Liu *et al* [13] observed activation of NF-κB through the non-canonical pathway in 65.2% of NKTLs in China, and these cases were associated with chemoresistance and poor prognosis. NF-κB activation has also been shown in NK cell lines, and treatment of tumour cells with NF-κB inhibitors (BAY 11–7082 and curcumin) resulted in the suppression of NF-κB activation and induction of apoptosis [33]. Our data indicate